Geological Society of America Bulletin

Neogene sediment structures in Bounty Trough, eastern New Zealand: Influence of magmatic and oceanic current activity

G. Uenzelmann-Neben, J. Grobys, K. Gohl and D. Barker

Geological Society of America Bulletin 2009;121;134-149
doi:10.1130/B26259.1

Notes

THE GEOLOGICAL SOCIETY OF AMERICA

Neogene sediment structures in Bounty Trough, eastern New Zealand: Influence of magmatic and oceanic current activity

G. Uenzelmann-Neben[†]
J. Grobys*
K. Gohl
Alfred-Wegener-Institute für Polar- und Meeresforschung, Postfach 120161, 27515 Bremerhaven, Germany

D. Barker
Institute of Geological and Nuclear Sciences, 69 Gracefield Road, Lower Hutt, New Zealand

ABSTRACT

New seismic reflection profiles have been interpreted to shed more light on the Neogene deposition in Bounty Trough, an aborted rift characterizing the eastern New Zealand continental margin. Two major processes influencing the deposition were identified. Magmatic activity led to the formation of basement highs, which deform the sedimentary sequences up to early and middle Miocene. The origin of the magmatism unfortunately cannot be solved with the new data presented here. It is difficult to say whether the magmatic activity is an on-going process. Drape structures in the youngest sedimentary unit argue against this. The Oligocene–Miocene represents a period of major change. Bottom current activity then took over as the most important depositional process. Strong cooling events in the late Miocene resulted in modification in the oceanographic regime east of New Zealand. This led to the formation of channels, sediment drifts, and sediment waves. At least since the Miocene, bottom current activity has been the dominating depositional process.

Keywords: Bounty Trough, seismic reflection profiles, basement highs, Neogene magmatic activity, bottom current activity, sediment drift.

INTRODUCTION

Bounty Trough, located on the eastern New Zealand continental margin (Fig. 1), constitutes a rift feature, which is bounded on the North by the Chatham Rise and on the South by the Campbell Plateau (Carter, 1988; Carter et al., 1994; Carter and Carter, 1996). Two N-S–oriented basement steps, the Inner and Outer Sills, divide Bounty Trough into three subbasins: the Inner Bounty Trough, the Middle Bounty Trough, and the Outer Bounty Trough (Carter et al., 1994, 1996). Davy (1993) defined those steps slightly differently as two zones of increased seafloor gradient (D1 and D2 in Fig. 1). Furthermore, he observed that zone D1 coincided with a change in strike direction of magnetic anomalies. The axis of Bounty Trough is occupied by one of the world's major deep-sea channel systems (Carter et al., 1994) and has been found to be the main transport path for terrigenous sediments from the South Island (McCave and Carter, 1997). Thus Bounty Trough acts as an archive for both the tectonic and climatic evolution of South Island, the adjacent Southern Ocean, and its eastern continental margin.

Inner Bounty Trough is underlain by block-faulted basement, which is interpreted to have originated as late Paleozoic to early Mesozoic oceanic crust (Carter et al., 1994; Carter and Carter, 1996). They interpreted rifting to have taken place along a previously established zone of basement weakness. Bounty Trough is thus interpreted as a rift within the eastern New Zealand continental margin before the start of spreading on the SW Pacific section of the mid-Pacific Rise (Carter, 1988; Davy, 1993). This theory is supported by Davy (1993), who concluded that the Cretaceous rifting followed trends that were inherited from Permian back-arc and/or oceanic crust formation. Sutherland (1999) observed a number of magnetic features in both Inner Bounty Trough and Middle Bounty Trough. The Inner Bounty Trough anomalies he correlated with structurally controlled igneous basement. He further won't rule out that the anomalies in Middle Bounty Trough are also the result of Cretaceous igneous activity.

While the tectonic origin of Bounty Trough is under strong discussion and several theories have been put forward, studies of the depositional environment have mainly concentrated on the head of Bounty Trough, where the Otago Fan gives information on the terrigenous sediment supply, and the Bounty Fan, where detailed information on the development of the Antarctic Circumpolar Current and the Deep Western Boundary Current can be gathered. Carter et al. (1994) presented in-strike lines across the Middle Bounty Trough. We here analyze two new seismic lines across the strike of Middle Bounty Trough and hence will address the climatic, oceanographic, and tectonic processes, which filled the aborted rift and shaped the sedimentary sequences. We will present evidence for a change in the main depositional process, which may be representative in general for the southern Pacific in the Neogene.

DATA ACQUISITION AND PROCESSING

In 2003 the Alfred Wegener Institute for Polar and Marine Research (AWI), in collaboration with the Institute for Geological and Nuclear Science (GNS), collected two seismic reflection profiles across the Middle Bounty Trough during RV *Sonne* cruise 169 (Fig. 1). For the western line AWI-20030002, a cluster of six Sercel G-guns™ with a total volume of 48 l (frequencies up to 150 Hz) was used as the seismic source, while three Sercel GI-guns™ (total volume the 2.2 l; frequencies up to 500 Hz) generated the seismic signal for the eastern line AWI-20030011. The data were received with a 180-channel streamer (2300 m long, Sercel Seal™ system). The data of line AWI-20030002 were recorded with a

[†]E-mail: gabriele.uenzelmann-neben@awi.de
*Present address: Federal Armed Forces Underwater Acoustic and Marine Geophysics Research Institute, Klausdorfer Weg 2-24, 24148 Kiel, Germany.

GSA Bulletin; January/February 2009; v. 121; no. 1/2; p. 134–149; doi: 10.1130/B26259.1; 12 figures; 1 table.

sampling rate of 4 ms, and a sampling rate of 1 ms was used for recording line AWI-290030011. The two seismic profiles were gathered with different acquisition parameters because line AWI-20030002 was gathered primarily as a crustal study (see Grobys et al., 2007) and the shots were recorded simultaneously with the streamer and ocean bottom seismometers, while line AWI-20030011 was set up to study the sedimentary sequences. Processing of the data comprised sorting (50 m common depth point [CDP] interval for line AWI-20030002; 25 m CDP interval for line AWI-20030011), a detailed velocity analysis to image the subsurface topography (every 50 CDPs), multiple suppression via a Radon transform filtering method, a spiking deconvolution to eliminate the bubble (a reverberation of the source signal), corrections for spherical divergence and normal moveout, application of streamer corrections, stacking, and migration. An Omega-X migration was carried out both in time and depth domain (Yilmaz, 2001). This method allows vertical variations in velocity and is accurate for large dips (≤85°, Yilmaz, 2001). The stacking velocities, which were converted into interval velocities using Dix's formula, were used to set up the velocity field used for the migration process and the embedded conversion from time to depth. The vertical resolution in time is a function of the recorded wavelength, which in turn is a function of the recorded frequency (Yilmaz, 2001). The recorded frequency is limited by the Nyquist frequency predetermined by the sampling rate. Having used temporal sampling rates of 4 ms for line AWI-2003002 and 1 ms for line AWI-20030011 during recording, the sampling rates in depth are 4 m and 1 m, respectively, using a velocity of 2000 m/s for the conversion.

To complement our data set, industry data and profiles acquired by GNS were made available to us for the interpretation.

STRATIGRAPHIC CONCEPT

Our seismic lines did not cross the locations of Deep Sea Drilling Project (DSDP) Leg 90 Site 594 and Ocean Drilling Program (ODP) Leg 181 Site 1122 (Fig. 1). Thus a direct tie of our seismic data to geological information was not possible. But a correlation with the seismostratigraphic concept developed by Carter et al. (1994) and Carter et al. (1999) led to the identification of four key reflectors. This identification is based on similarities in reflection characteristics of both the seismic horizons and units.

The oldest identifiable reflector is interpreted as the top of the basement (Fig. 2). The reflection shows a strong amplitude, in general a good continuity with a rough, rugged topography and forms the top of a layer, which can be resolved only in a few places. We observe a few strongly dipping internal reflections that can be traced for a few kilometers. They overlap and are superposed to form subparallel-stratified sequences. In character, those reflections are not unlike those associated with lava flows in extensional volcanic provinces (e.g., Uenzelmann-Neben et al., 1999). The basement was not drilled in either DSDP or ODP sites. Hence nothing is known about the age of the basement. But both Carter et al. (1994) and Carter et al. (1999) assume the basement to be of oceanic origin.

The unit on top of the basement, unit D, shows a number of internal reflections, which are much stronger in the upper 200–300 m (Fig. 2 and Table 1). The unit shows a thickness between 200 m and 600 m. According to Carter et al. (1994) and Carter et al. (1999), unit D comprises the postrift sedimentary cover and is of Cretaceous to Paleocene age. The top of unit D is formed by a strong, slightly rugged reflector (Fig. 2). It shows good continuity and is correlated with reflector W of Carter et al. (1994).

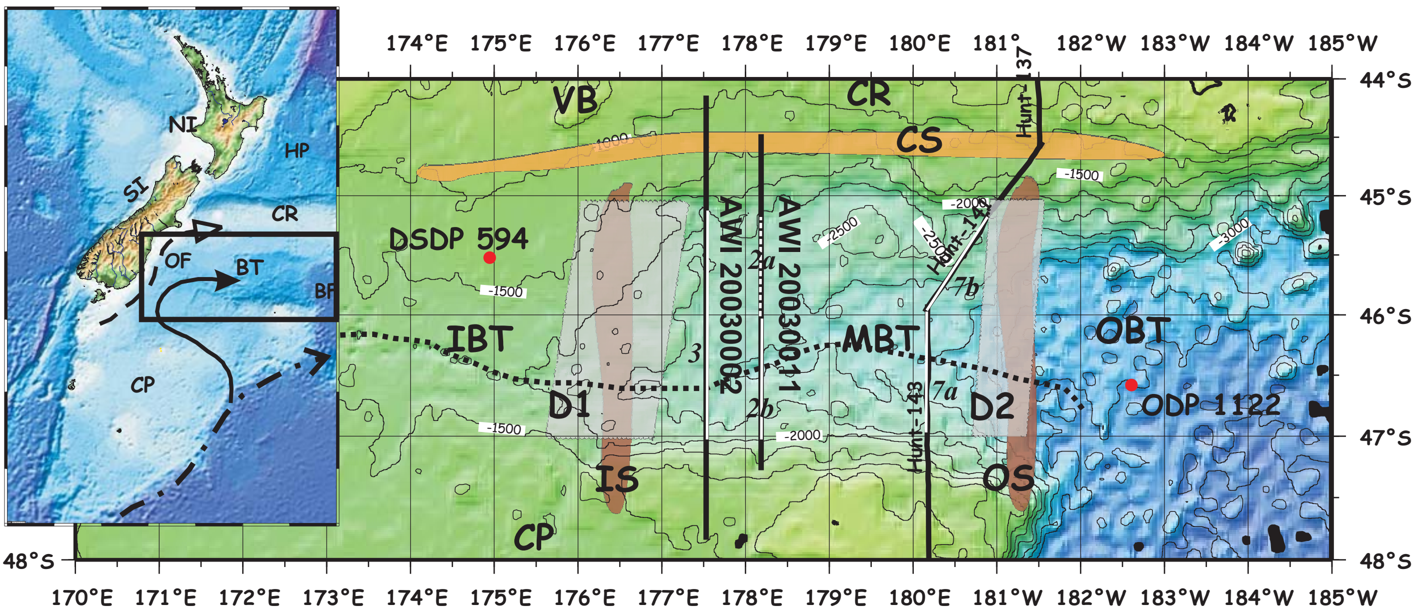

Figure 1. Satellite-derived predicted bathymetric (Smith and Sandwell, 1997) map of the eastern New Zealand (inset map) and the Bounty Trough. The locations of Deep Sea Drilling Project (DSDP) Site 594 and Ocean Drilling Program (ODP) Site 1122 are included. The dotted line shows the trace of the Bounty Channel. The white lines and italic numbers refer to the parts of lines AWI-20030002, AWI-20030011, Hunt-A143, and Hunt-A141 displayed in Figures 2, 3, and 7. BF—Bounty Fan; BT—Bounty Trough; CP—Campbell Plateau; CR—Chatham Rise; CS—Chatham Sill; D1 and D2—bathymetric steps according to Davy (1993); HP—Hikurangi Plateau; IBT—Inner Bounty Trough; IS—Inner Sill; MBT—Middle Bounty Trough; NI—North Island; OBT—Outer Bounty Trough; OF—Otago Fan; OS—Outer Sill; SI—South Island; VB—Veryan Bank. Line 137/141/143 is from Davy (1993). The inset map shows the paths of the Antarctic Circumpolar Current (dot-dashed), a local gyre (bold), and the Southland Current (dashed).

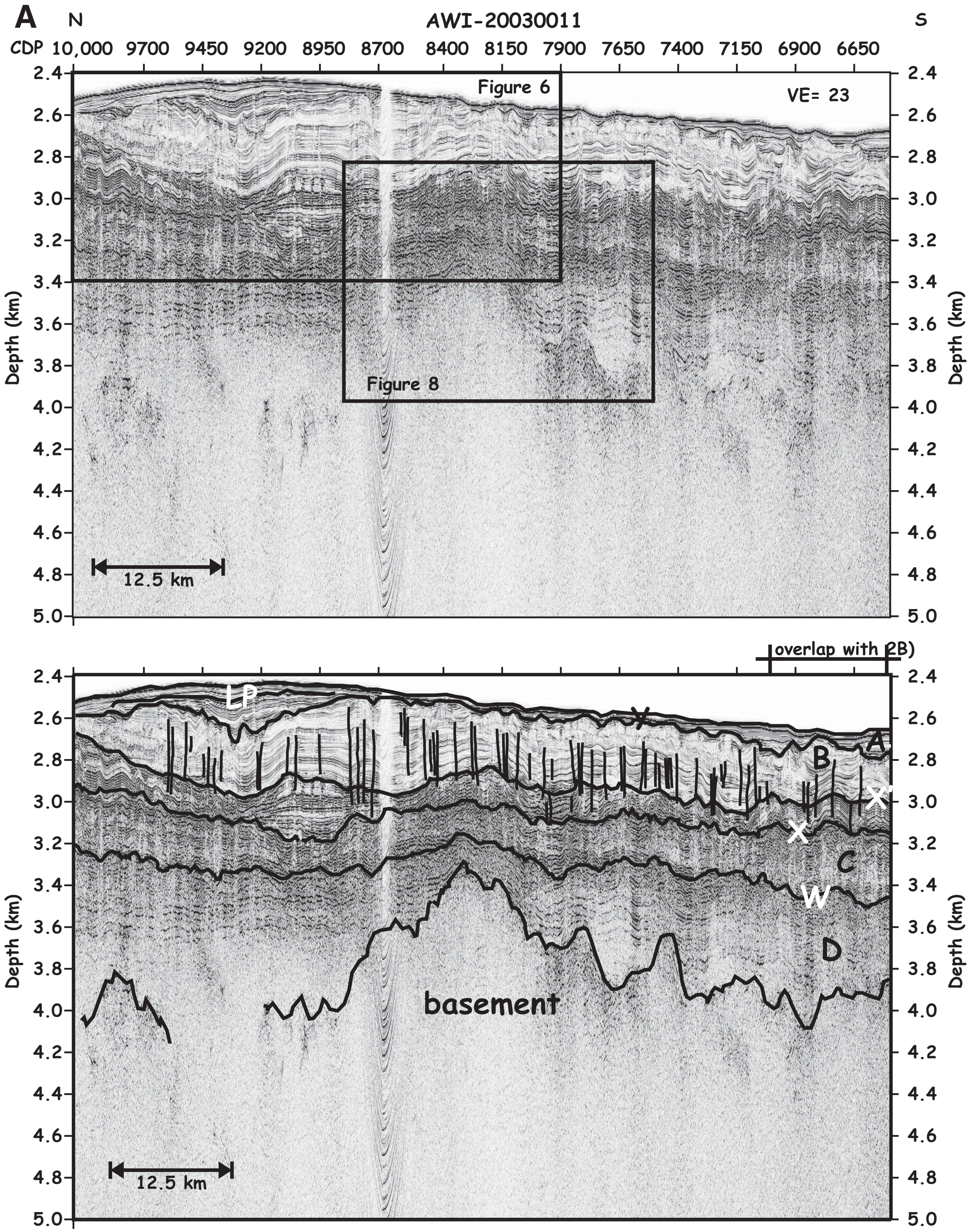

Figure 2. Line AWI-20030011. The boxes show the location of the blown-up part in Figures 5, 6, 8, and 10. For location, see Figure 1. (A) Northern part of the line; (B) southern part of the line. (*Continued on following page*.)

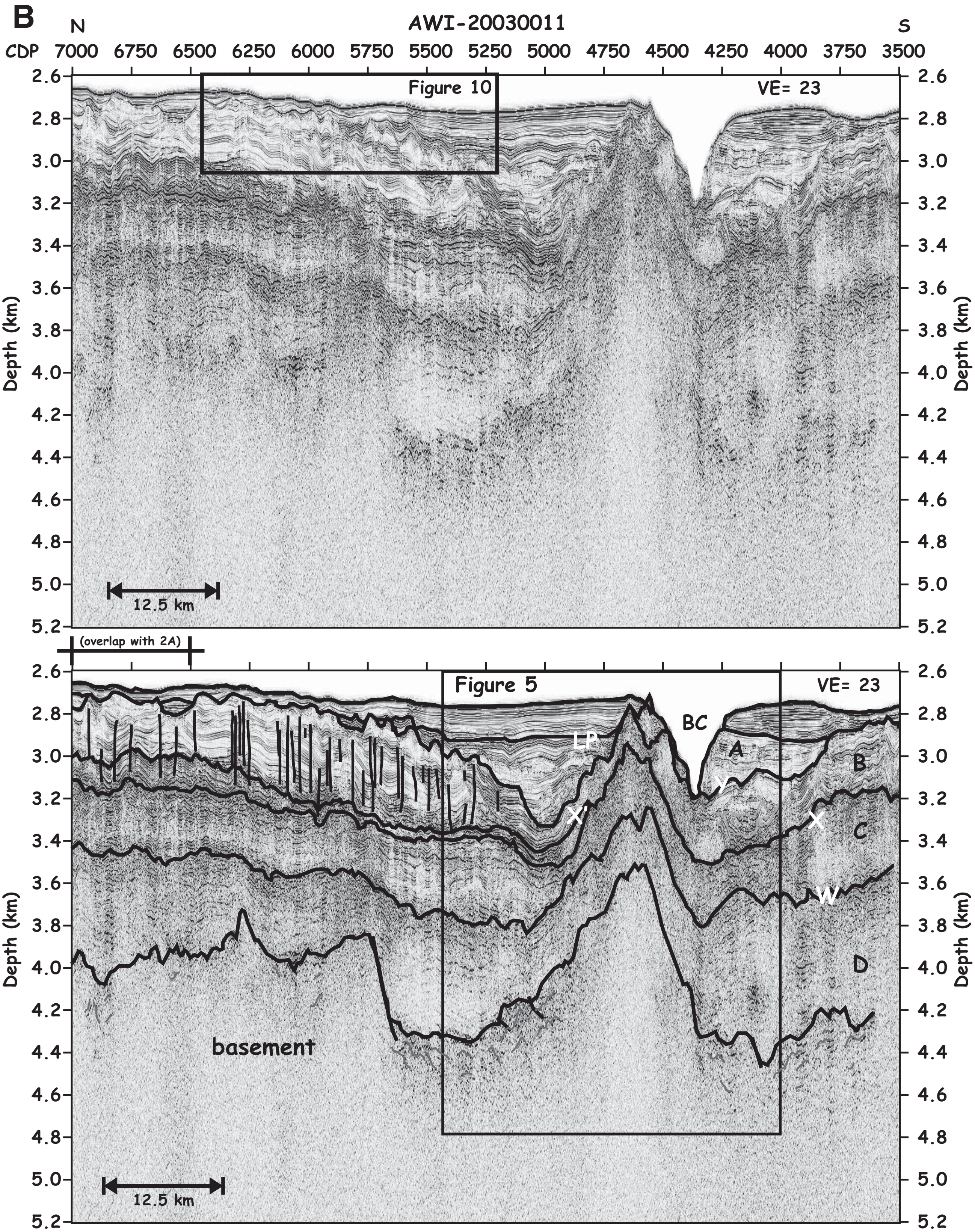

Figure 2 (*continued*). Note the strong basement high immediately north of the Bounty Channel (BC). Vertical black lines—small-scale faults probably as the result of differential compaction; A/B/C/D—units A–D. Abbreviations: CDP—common depth point; VE—vertical exaggeration.

TABLE 1. SEISMOSTRATIGRAPHIC CONCEPT FOLLOWING CARTER ET AL. (1994) AND CARTER ET AL. (1999)

Reflector or unit	Character	Age	Thickness	Origin
Top basement	Strong amplitude, good continuity, rugged topography			oceanic
Unit D	Internal reflections	Cretaceous–Paleocene	200–600	Post-rift sediments
Reflector W	Good continuity	Paleocene		
Unit C	Strong internal reflections, lower part transparent	Eocene–Oligocene	200–400	
Reflector X	Strong, continuous, local erosion	Mid-Oligocene		Marshall Paraconformity
Unit B	Strong internal reflections in lower part, upper part weaker, change ≡ reflector X'	Mid-Oligocene–late Miocene (>8.5 Ma)	200–600	
Reflector Y	Continuous, medium strength, strong evidence of erosion	Late Miocene (8.5–6.5 Ma)		
Unit A	Strong parallel internal reflections, onlap onto unit B	Late Miocene (6.5 Ma)–Recent	Up to 600 m	

Unfortunately, this reflection was not drilled at Site 594. Reflector W has been assigned a tentative age of Paleocene by correlation to exploration drill holes on the nearby Canterbury Shelf and Great South Basin (Carter et al., 1994).

Unit C, on top of reflector W, is 200–400 m thick and shows strong internal reflectors in the upper part (Fig. 2 and Table 1). The lower part of the unit tends to acoustic transparency. This unit has been assigned an age of Eocene to Oligocene by Carter et al. (1994). The top of unit C is formed by a strong continuous reflection, which locally shows erosion (e.g., Fig. 2, CDPs 3500–3750, 3900–4400, 5700–6000, 7100–7800, 8000–8700, and 9300–10,000). Because of its erosive character we correlate this reflector with reflector X of Carter et al. (1994). They assumed reflector X to represent the Marshall Paraconformity (Table 1), a widespread feature throughout the New Zealand Plateau and beyond (Fulthorpe et al., 1996). This paraconformity may have resulted from a mid-Oligocene sea-level fall and increased current activity (e.g., the evolving Antarctic Circumpolar Current) as a result of the opening of the Tasman gateway (Carter et al., 1994; Fulthorpe et al., 1996). ODP Leg 181 showed the latter to be more likely (Carter et al., 1999).

Unit B shows strong continuous internal reflections in the lower part and weaker, but still continuous internal reflectors in the upper part (Fig. 3). This change in reflection amplitude is very distinct and may be correlated with reflector X′ of Davy (1993) (Fig. 2). Furthermore, onlaps onto this horizon can be observed (Fig. 2, e.g., CDP 6400 and 6100) indicating not only a change in sedimentation environment but also a period of erosion or nondeposition. Davy (1993) considered this reflector to mark the Oligocene–Miocene boundary. Unit B was drilled at DSDP Leg 90 Site 594 and found to be of mid-Oligocene to late Miocene (>8.5 Ma) age (Shipboard Scientific Party, 1986). Unit B is 200–600 m thick on our lines, it thins toward the east, and is absent at ODP Leg 181 Site 1122 on the Bounty Fan (Carter et al., 1999) (Table 1).

A continuous reflection of medium strength, which we correlate with reflector Y of Carter et al. (1994), forms the top of unit B. This reflection shows strong evidence of erosion cutting repeatedly into unit B (e.g., Fig. 2, CDPs 3800–3950 and 5700–6650). The overlying unit A shows onlap onto this reflection (Fig. 2, CDPs 5000–5700 and 8700–9700). Reflector Y was penetrated at DSDP Leg 90 Site 594 and found to be of late Miocene age (8.5–6.5 Ma) (Shipboard Scientific Party, 1986).

The youngest unit A shows strong parallel reflections. This unit drapes and onlaps reflector Y and unit B (Fig. 2). Unit A comprises the levees of Bounty Channel (Carter and Carter, 1988) and it is up to 600 m thick. Unit A was drilled at DSDP Leg 90 Site 594 and found to be of late Miocene (6.5 Ma) to Recent age (Shipboard Scientific Party, 1986) (Table 1). At ODP Leg 181 Site 1122 unit A was found to comprise sediments of mid-Miocene (16.7 Ma) to recent age (Carter et al., 1999). This discrepancy in age may be a result of additional sediment transported to Site 1122 via the Deep Western Boundary Current, which cannot be detected within Bounty Trough.

OBSERVATIONS

Basement Structures

The seismic data show an up to 2000-m-thick accumulation of well-stratified sediments within the Middle Bounty Trough (Figs. 2 and 3). The stratigraphic concept suggests that the sediments date back to the Cretaceous.

The basement itself is characterized by several highs. Line AWI-20030002 shows two uparching structures, which originate in the basement (Fig. 3, CDPs 3600–4700). Here, the top basement reflector is disrupted and not continuous. It shows a strong reflection amplitude where traceable. The bodies forming the highs show a very low internal signal-to-noise ratio implying homogeneous material. The anticlines are separated by a ~12-km-wide depression. The uparching structures are 12–25 km in width at their base and ~200 m high. Seismic interval velocities increase from below 3900 m/s within sedimentary units D to A to more than 5700 m/s for the basement (Fig. 4B, bluish-greenish colors v_{int} <3900 m/s, orange color v_{int} >5700 m/s). The uparching structures observed in the seismic data can be identified in the velocity data as well (Fig. 4B). Thus we infer that the basement highs represent igneous material, akin to the basement material. This is supported by a *P*-wave velocity model inferred from wide-angle/refracted data along line AWI-20030002 (Grobys et al., 2007). The sedimentary units D and C follow the basement highs in their morphology (Figs. 3 and 4A, CDPs 3600–4700). The basement highs do not show a base reflection. A leveling of the morphology of the highs cannot be observed in the sediments, nor do we observe an infill of the depression. The sediments do not onlap the highs. Only slight changes in the thickness of the unit appear. No smoothing of the features nor significant decrease in horizon dip can be seen in the younger units. In general, reflector W is easy to trace and only partly disrupted over the basement highs (Fig. 4A, CDPs 3800–3900, 3950–4050, and 4450) and at their flanks (Fig. 4A, CDPs 4180 and 4550). Reflector X is more difficult to trace and shows stronger disruption over the basement highs (Fig. 4A, CDPs 3800–3900, 4000–4080, 4200–4300, and 4450). Especially CDPs 4000–4080 and 4450 show erosional character (Fig. 4A). Reflector Y shows a good continuity across the basement highs and is easy to trace. This reflector appears to be affected by erosion especially above the basement highs, and the unit thins toward the highs (Fig. 4A). We observe strong erosion in the younger part of unit B. Those characteristics all point to synsedimentary and/or post-sedimentary deformation rather than sediment drape.

Line AWI-20030011, located farther east, shows a significant basement high immediately north of the Bounty Channel (Figs. 2 and 5A, CDPs 4300–4800). The high is ~10 km wide at its base and ~600 m high. Again, we observe

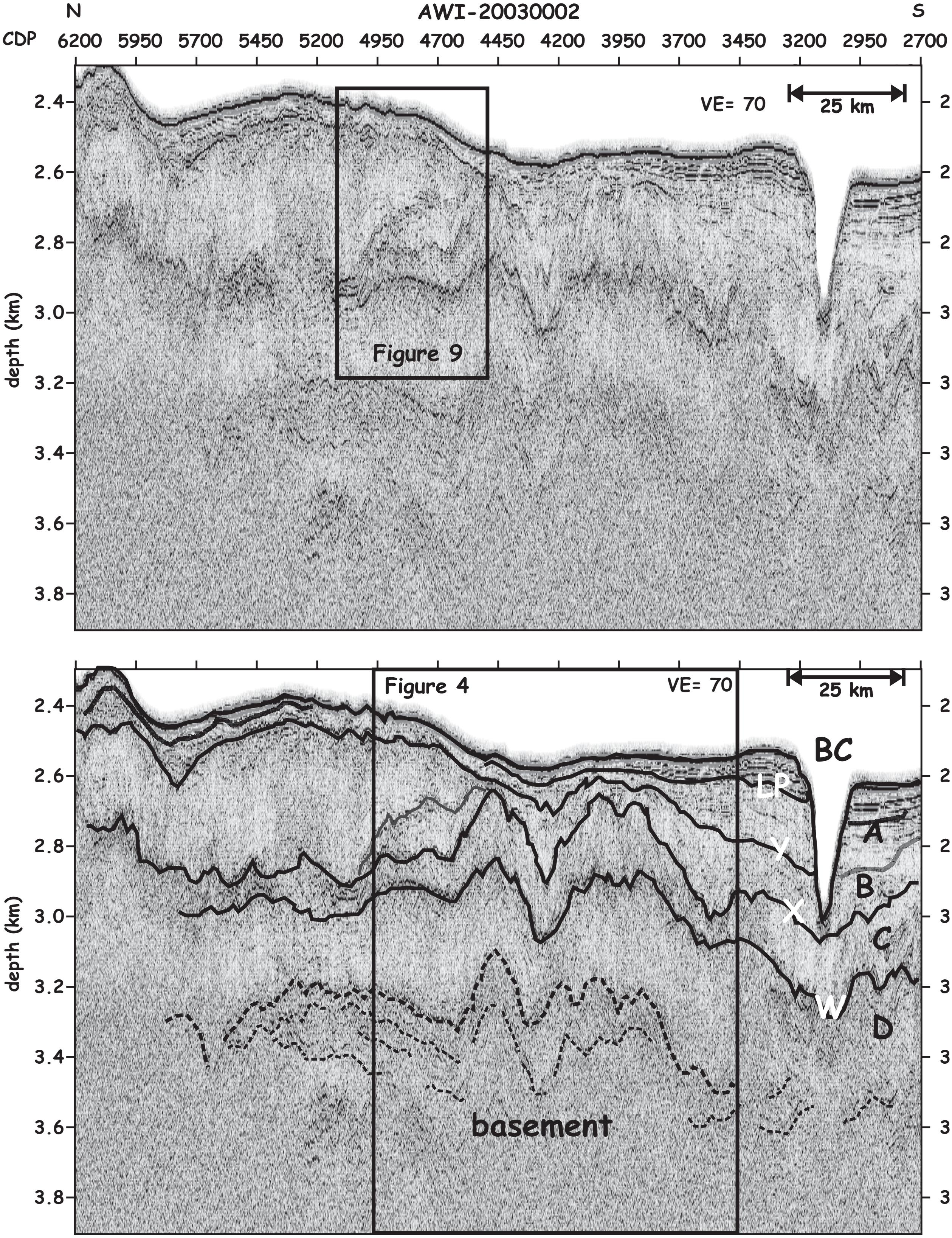

Figure 3. Line AWI-20030002. The boxes show the location of the blown-up part in Figures 4 and 9. For location, see Figure 1. Vertical black lines—small-scale faults probably as the result of differential compaction; A/B/C/D—units A–D; BC—Bounty Channel. Abbreviations: CDP—common depth point; VE—vertical exaggeration.

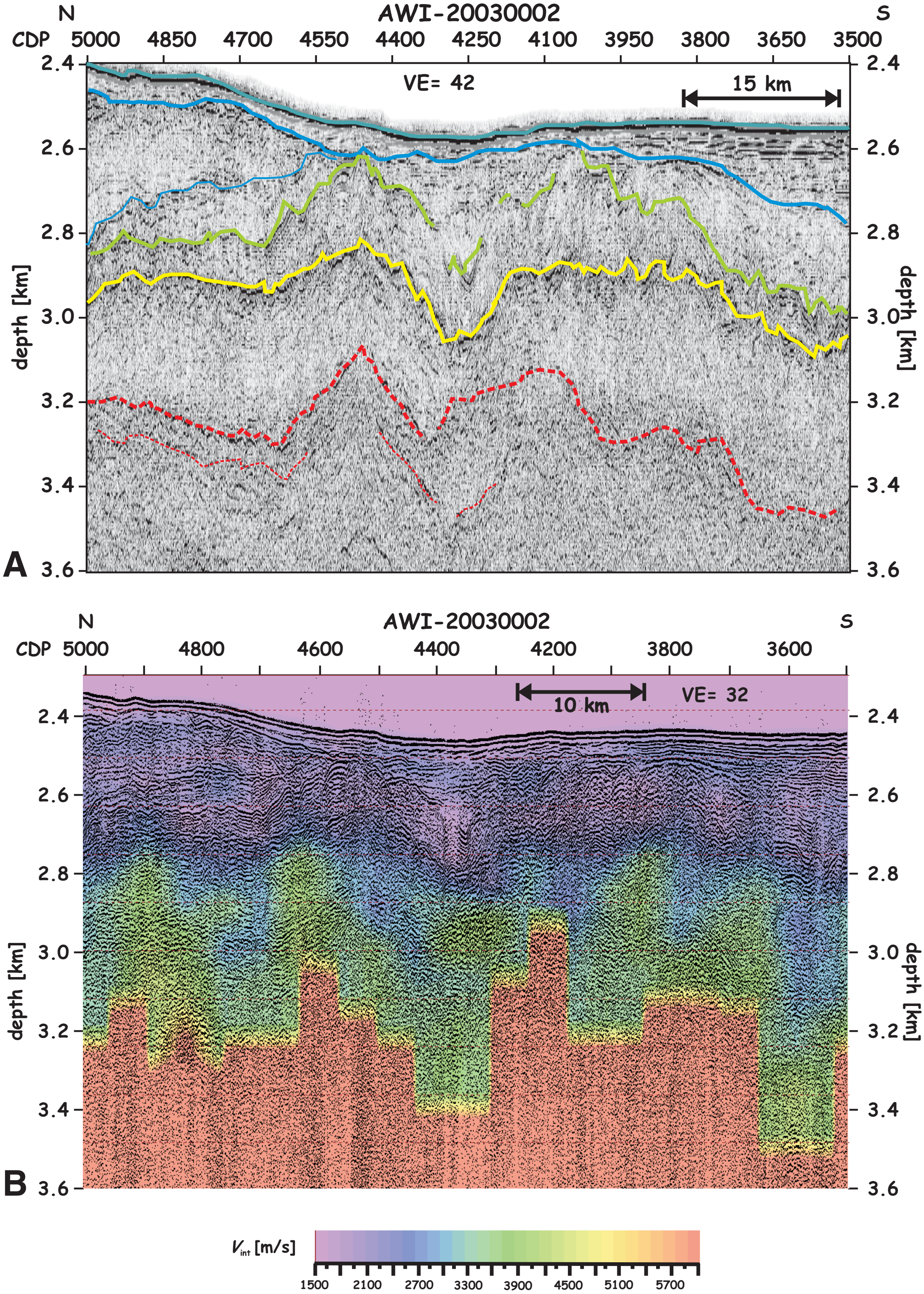

Figure 4. Blow-up of line AWI-20030002, CDPs 3500–5000 showing the basement high, the form of which is well repeated at least up to reflector X. For location, see Figure 3. (A) Seismic section with interpretation. Light green line—seafloor; purple line—reflector LP late Pleistocene; petrol line—reflector Y; dark green line—reflector X; yellow line—reflector W; red line—top of basement. (B) Seismic data overlain by interval velocity field v_{int}. Note the distinct increase in v_{int} from values below 4800 m/s (greenish-bluish colors) to values above 6000 m/s (orange color) interpreted to represent the top of basement. This velocity horizon shows a doming that parallels the interpreted rise in the basement. Abbreviations: CDP—common depth point; VE—vertical exaggeration.

an uparching in the high seismic velocities >5700 m/s (Fig. 5B, bluish-greenish colors v_{int} <3900 m/s, orange color v_{int} >5700 m/s) indicating igneous material for the basement high. The sedimentary units up to unit B follow the morphology of the basement high. Across the high, the sedimentary units thin: from ~550 m, unit D thins to 220–300 m above the high, unit C thins from ~300 m to 200–280 m, and unit B shows a thinning from ~580 m to 100–300 m. Units D–B do not onlap the basement high, but we observe onlap of unit A onto unit B (Figs. 2 and 5A, CDPs 3800–4300 and 4700–5400). Reflector Y shows strong erosion via truncation of the internal reflectors at the top. We observe both toplap and lateral truncation at the top of unit B. Younger reflections onlap reflector Y characterizing it as an unconformity. Reflector Y shows small-scale topography (Fig. 2, CDP 5200–7000) with small depressions filled by unit A. Only the uppermost, youngest part of unit A covers the basement high and hence is slightly deformed.

In the northern part, line AWI-20030011 shows another basement high (Figs. 2A and 6, CDPs 7500–9000). In contrast to the one near the Bounty Channel and the two highs on line AWI-20030002, the topographic effect of this basement high is nearly compensated for by unit D sediments. The oldest sediments of unit D show onlap onto the high, and the morphology has already been leveled by sediments of unit D. Unit C only slightly images the high, and it is no longer detectable in unit B. Hence, we conclude that this high was formed pre-sedimentary.

Farther in the east, line Hunt-143 shows two smaller basement highs, one with flow structures toward the north (Fig. 7A). A deformation of the sediments due to those highs is not detectable in the sedimentary units. Line Hunt-141 shows another basement high in the northern part of the Bounty Trough (Fig. 7B). The northern high on line AWI-20030011 shows onlap of the sedimentary horizons in unit D and a leveling effect in units C–A, although the morphology of the high still can be seen in the seafloor topography.

Sedimentary Sequences

Sedimentation of units D and C appears to have been relatively undisturbed. With a few exceptions (Fig. 2, CDPs 4300–5100; Fig. 3, CDPs 3700–4600) unit D drapes over the basement topography and fills the depressions between smaller local basement highs. We observe onlap onto the basement (Fig. 2, CDPs 7500–8000 and 8200–8700; Fig. 7A, CDPs 8600–9800; Fig. 7B, CDPs 5000–5600 and 6500–7100) as well as reductions in unit thickness across basement highs (Fig. 2, CDPs 5400–5800 and 6900–9200; Fig. 7A, CDPs 5900–7100). For unit C, thickness variations as well as leveling and onlap onto unit D can be observed (Fig. 2, CDPs 5000–6000; Fig. 7B, CDPs 5000–7000). We observe a drape and smoothing-out of basement structures except for those mentioned above. Both reflectors W and X show a small-scale topography with lateral and toplap termination of internal reflectors indicating erosion. Above the observed basement highs, reflectors W and X are disrupted (Figs. 2 and 3).

We observe a distinct change in reflectivity within unit B: strong internal reflections in the lower part, weaker reflectivity in the upper part. Carter et al. (1994) correlated this change with the transition from the Kekenoden group, corresponding to the maximum flooding platform, to the Otakou group, representing nonorogenic progradation. Within the lower unit B we can identify two distinct sedimentary bodies (Fig. 5A, CDPs 4850–4900; Fig. 8, CDPs 9300–10,200; Fig. 9, CDPs 4500–5000). Those sedimentary bodies show an asymmetric geometry with both a steep and a gentle flank. Transparent layers alternate with continuous strong reflections (Fig. 8). Internal reflections are truncated abruptly (Figs. 8 and 9). Those characteristics correspond to the ones reported for sediment drifts (Uenzelmann-Neben, 2001; Stow et al., 2002). Both sediment drifts appear to be patched onto the slope of Chatham Rise (Fig. 8) and the doming related to the basement high in the central Bounty Trough (Fig. 9). Hence, the sediment drifts are considered to belong to the group of channel-related patched drifts. The internal reflections of upper unit B show onlap onto the drifts.

Upper unit B shows a number of small-scale faults (black lines in Figs. 2 and 3). These are interpreted as the result of differential compaction due to rapid sediment deposition. Within this part of the unit we also observe a sedimentary body characterized by a mounded geometry and subparallel internal reflections (Fig. 2, north of CDP 5700; Fig. 3, north of CDP 4500). We can interpret both transparent layers and strong reflectors (Fig. 8). On the basis of those reflection characteristics, we identify this sedimentary body as another sediment drift. We observe a moat between this drift and the rise toward Chatham Rise and a number of channels (Fig. 2, CDPs 5000–5350, 5400–5600, and 6900–7000; Fig. 8, CDPs 10,100–10,200) and infill structures. Levees or overbank deposits in connection with the channels cannot be identified. The upper part of unit B is missing across the basement highs on line AWI-20030002 (Figs. 3 and 4A, CDPs 3800–4700). The lateral and top termination of the internal reflectors against reflector Y indicates erosion. Unit A then drapes over this structure.

A number of acoustically transparent bodies can be observed in unit B (Fig. 5A, CDPs 4000–4180, 4250–4350, 4450–4500, and 4800–4950). Those show no internal reflections and a rather chaotic structure.

Reflector Y, which forms the top of unit B, shows evidence for strong erosion. Unit A onlaps this reflector and fills and drapes over its topography. In places, sediment waves can be observed (Fig. 10, CDPs 5900–6400) both in reflector Y as well as in sediments of unit A. Unit A comprises the levees of the Bounty Channel (Carter and Carter, 1988). No indications for the channel at its present location can be found in unit B.

TECTONIC IMPLICATIONS

We observe two types of basement highs: (1) those for which topographic relief is preserved in overlying sedimentary units—at least up to unit B, and (2) those for which the topography has been rapidly erased by drape. There are several possible origins of the basement highs: (1) pre-sedimentary basement block faulting as a result of Cretaceous rifting, (2) Tertiary igneous intrusions along Cretaceous faults, and (3) Neogene salt or mud diapirism. If the basement highs were pre-sedimentary, the sedimentary units would show a drape. We would expect features such as onlap of the sedimentary horizons onto the highs, a leveling and/or smoothing of the morphology of the highs, a decrease of the dips of internal reflections, and/or infill in depressions between highs. We observe onlap onto the basement highs, a leveling and/or smoothing of the morphology of the highs, and variations in the thickness of the sedimentary units as well as a drape of the sedimentary units across the highs for a few basement structures on lines AWI-20030011 (Figs. 2A and 6, CDPs 7500–9000), Hunt-143 (Fig. 7A, CDPs 8000–10,100), and Hunt-141 (Fig. 7B, CDPs 5000–7400). We hence interpret those basement highs as pre-sedimentary.

We do not recognize any of the expected features for the other basement highs observed on lines AWI-20030002 (Fig. 3, CDPs 3600–4700) and AWI-20030011 (Fig. 2, CDPs 4300–4800). There, we observe disruption of both basement and sedimentary reflectors and only slight variations in thickness of the sedimentary units D, C, and B. The morphology of the sedimentary units follows the basement morphology. This points to a post-sedimentary deformation. Since unit B (middle Oligocene–late Miocene) is affected as well, we propose that this process took place in the middle to late Miocene.

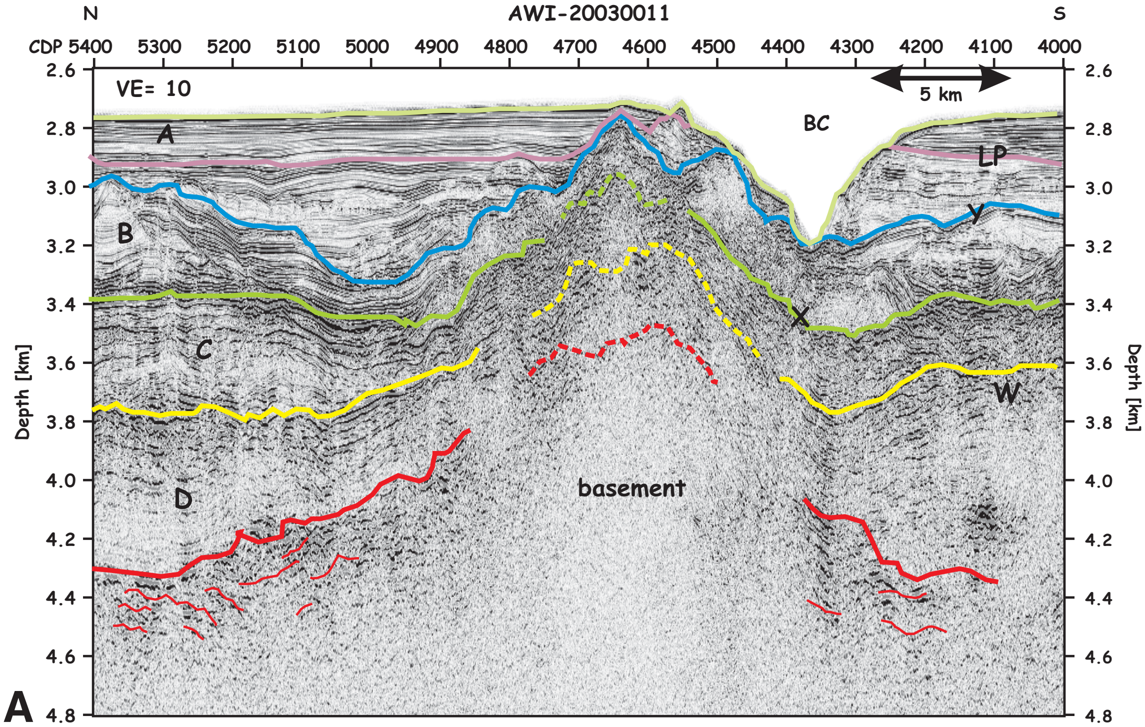

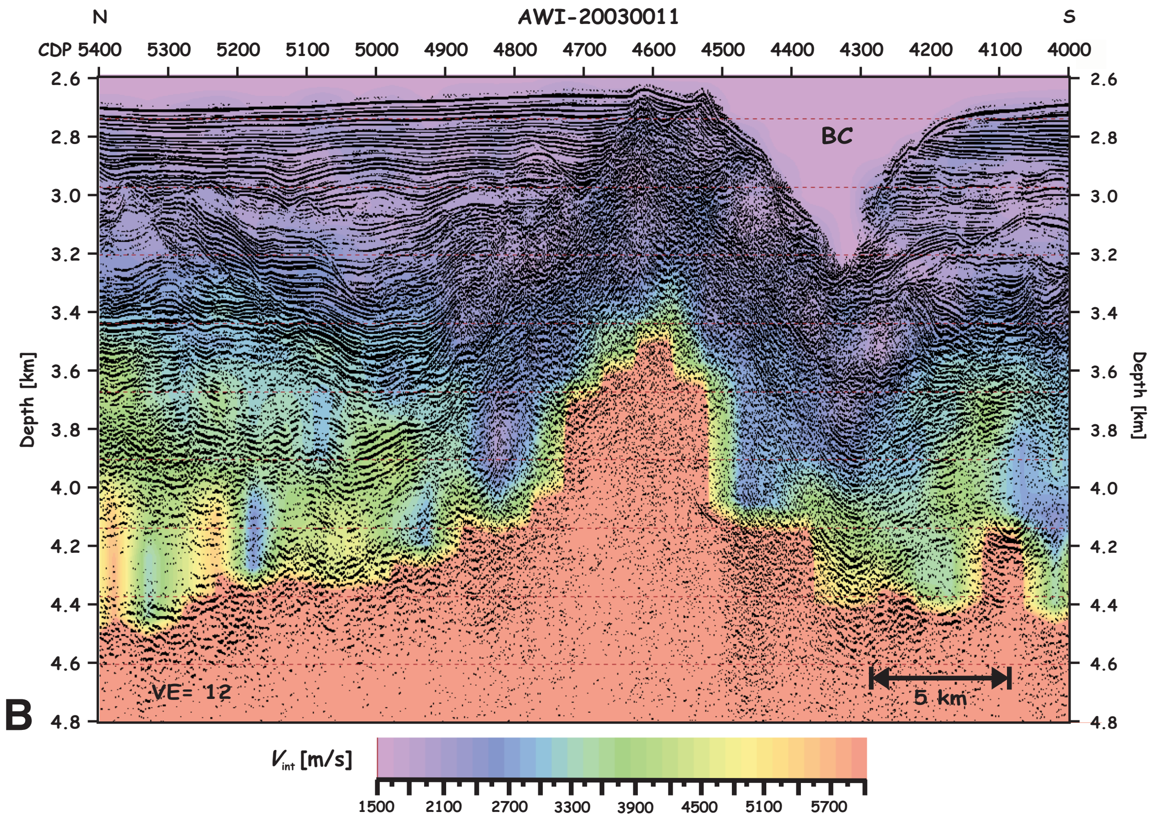

Figure 5. Part of line AWI-20030011. For location, see Figure 2. (A) Seismic data with interpretation. Note the strong basement high immediately north of the Bounty Channel (BC). Light green line—seafloor; purple line—reflector LP late Pleistocene; petrol line—reflector Y; dark green line—reflector X; yellow line—reflector W; red line—top of basement; vertical black lines—small-scale faults probably as the result of differential compaction; A/B/C/D—units A–D. (B) Seismic data overlain by interval velocity field v_{int}. Note the distinct increase in v_{int} from values below 4800 m/s (greenish-bluish colors) to values above 6000 m/s (orange color) interpreted to represent the top of the basement. Note the rise in this velocity horizon, which fits the interpreted basement high.

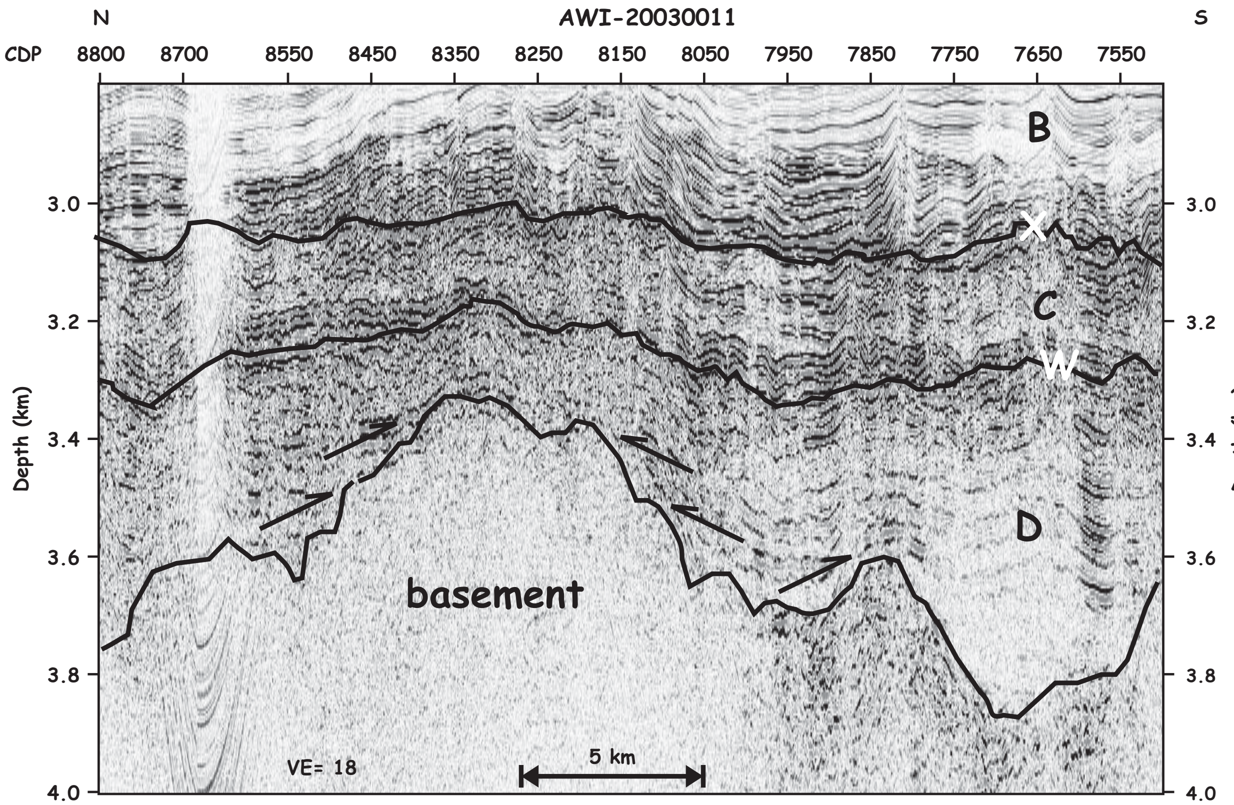

Figure 6. Blow-up of line AWI-200300011 showing the basement high between common depth points (CDPs) 7500 and 8800 with onlaps onto the basement high. For location see Figure 2. Reflector X′ according to Davy (1993); vertical black lines—small-scale faults probably as the result of differential compaction; A/B/C/D—units A–D. VE—vertical exaggeration. For age and origin of the reflectors, see Table 1.

Diapirism could result in deformed sequences. However, salt diapirism would require a salt basin in Bounty Trough for which there is no evidence. Furthermore, a salt diapir would not originate in the basement (Stewart et al., 1996; Selly, 1997), as the observed structures do, and should show a distinct negative gravity anomaly. We observe positive gravity anomalies of 20–25 mgal across the basement highs in question (Fig. 11, green to yellow-red colors) (Smith and Sandwell, 1997). The gravity high across the basement highs located on line AWI-20030002 (Fig. 3, CDPs 3600–4700) was investigated by Gobys et al. (2007) (their Fig. 16). They used a high-density body in the lower crust to model the gravity anomaly. This lower crustal, high-density body was ascribed to a mafic intrusion, which can also be observed in the velocity model of Grobys et al. (2007) (their Figs. 15 and 16) and correlates with magnetic anomalies. Mud diapirism requires rapid sedimentation rates leading to overpressure in the sequence and hence fluid and mud expulsion. No indications for extremely high sedimentation rates in sedimentary unit D or older were found. Therefore, we rule out mud or salt diapirs as the origin of the highs.

Magnetic data show an anomaly (–150 nT) over the high on line AWI-20030011 immediately north of Bounty Channel (Davy, 2005, personal commun.). Magnetic anomalies are not that well defined for the other highs (bold circles in Fig. 12), but other magnetic features do not show up in the magnetic structures map either, e.g., the volcanics at the Otago and Banks Peninsulas (bold squares in Fig. 12). However, since the seismic velocities of the highs resemble those of the basement (Figs. 4B and 5B), we conclude that the highs represent igneous material. Furthermore, the structure of the basement highs (tall, upright seismic dead zones, upturned host rocks, and uplifted overburden) qualifies them as vertical intrusions (Lee et al., 2006). The areal distribution of the magmatic structures indicates that the intensity decreases toward the east. The locations of the structures correlate with positive anomalies in the satellite gravity map (Fig. 11) (Smith and Sandwell, 1997). Unfortunately, this does not apply to the Inner and Outer Sills, and is ambiguous for the Chatham Sill, although the Chatham Sill was associated with submarine activity in late Miocene and Pliocene times (Carter et al., 1994).

Other Miocene and Pliocene intraplate volcanics (Veryan Bank, Mernoo Bank, and Urry Knolls) are nearby (Fig. 11) (Wood et al., 1989). Additionally, Davy (1993) observed a number of intrusions in the area between 179° E and 179° W. Carter et al. (1994) traced back the top of the youngest affected sequence, reflector Y, to a tectonic (volcanic and folding) origin and related it with (1) the eruption of alkaline volcanics at Banks and Otago Peninsulas, (2) late Miocene tectonism und unconformity cutting in eastern Otago, (3) intrusive volcanism along the southern slopes of Chatham Rise, the Urry Knolls, and south of Chatham Island, (4) a change in direction of plate motion along the Alpine transform at ca. 10–8 Ma from dominantly strike-slip to strongly transpressive, and (5) erosion as a secondary effect to shape reflector Y due to an intensification of major bottom

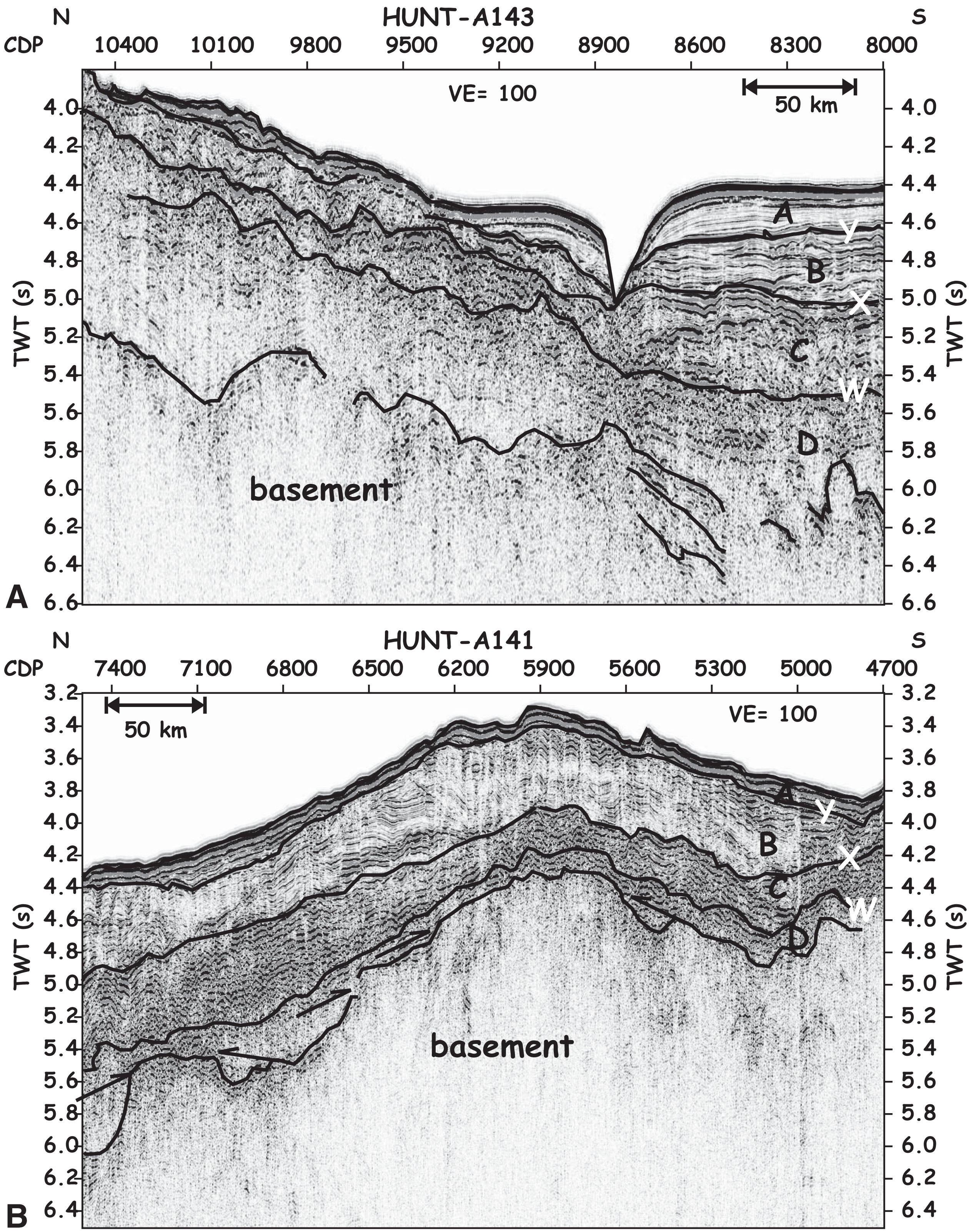

Figure 7. (A) Part of line Hunt-A143. For location, see Figure 1. Note the small basement high in the vicinity of the Bounty Channel (BC). (B) Part of line Hunt-A141. Note the onlaps onto the basement high as shown by the black arrows. Reflector X′ according to Davy (1993); vertical black lines—small-scale faults probably as the result of differential cmpaction. A/B/C/D—units A–D. For age and origin, see Table 1. Abbreviations: CDP—common depth point; TWTT—two-way travel time; VE—vertical exaggeration.

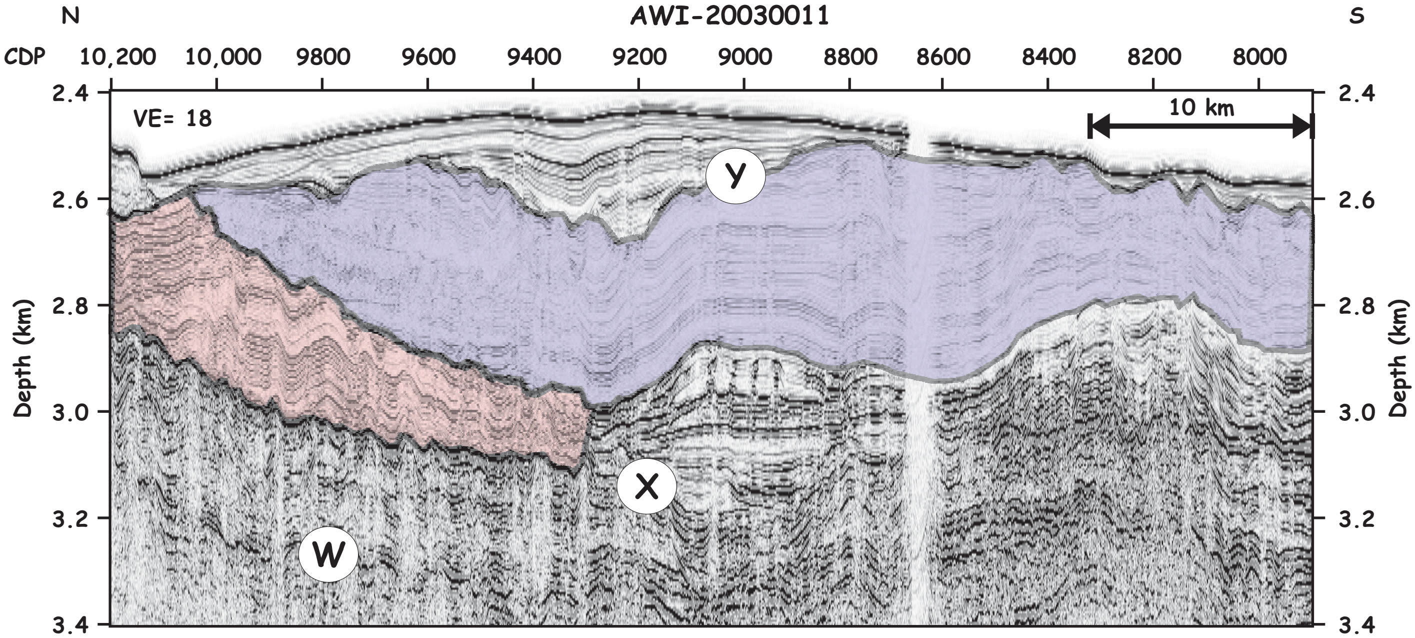

Figure 8. Blow-up of line AWI-20030011 showing the sediment drifts within unit B with pink outlining the older and purple the younger sediment drift. For location, see Figure 2. A/B/C/D—units A–D. CDP—common depth point.

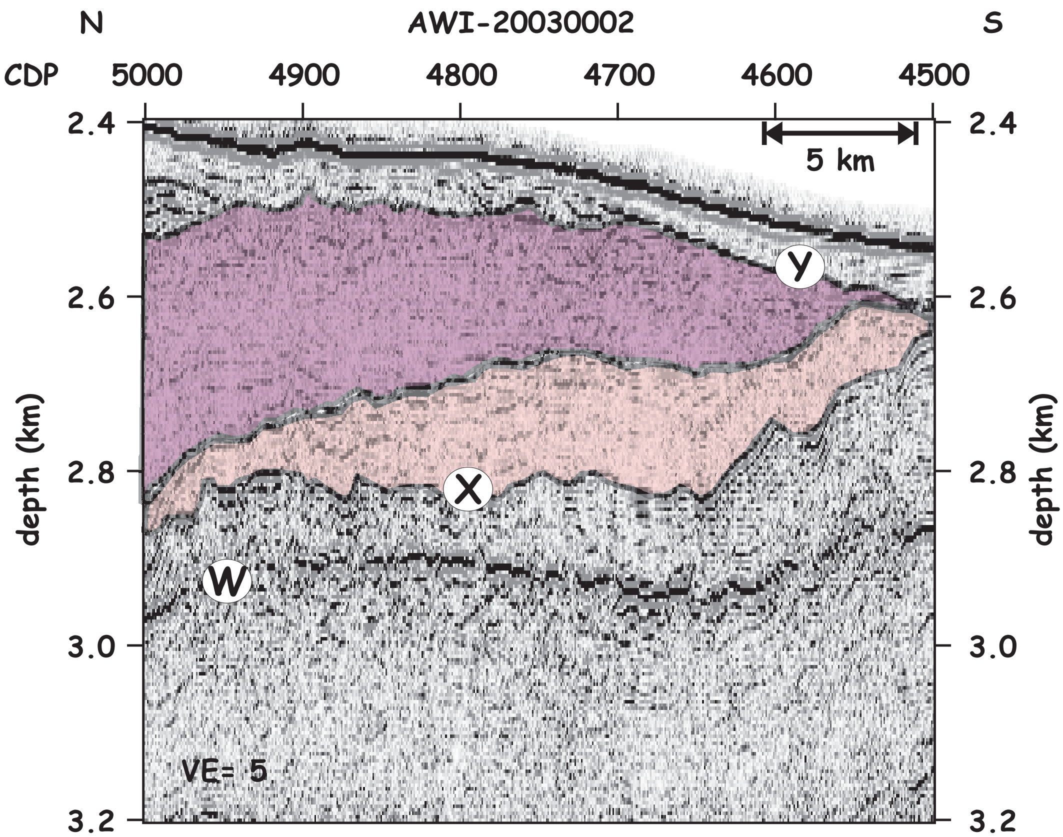

Figure 9. Blow-up of line AWI-20030002, common depth point (CDP) 4500–5000 outlining the sediment drifts in unit B (pink—older drift; purple—younger drift). For location, see Figure 3. CDP—common depth point.

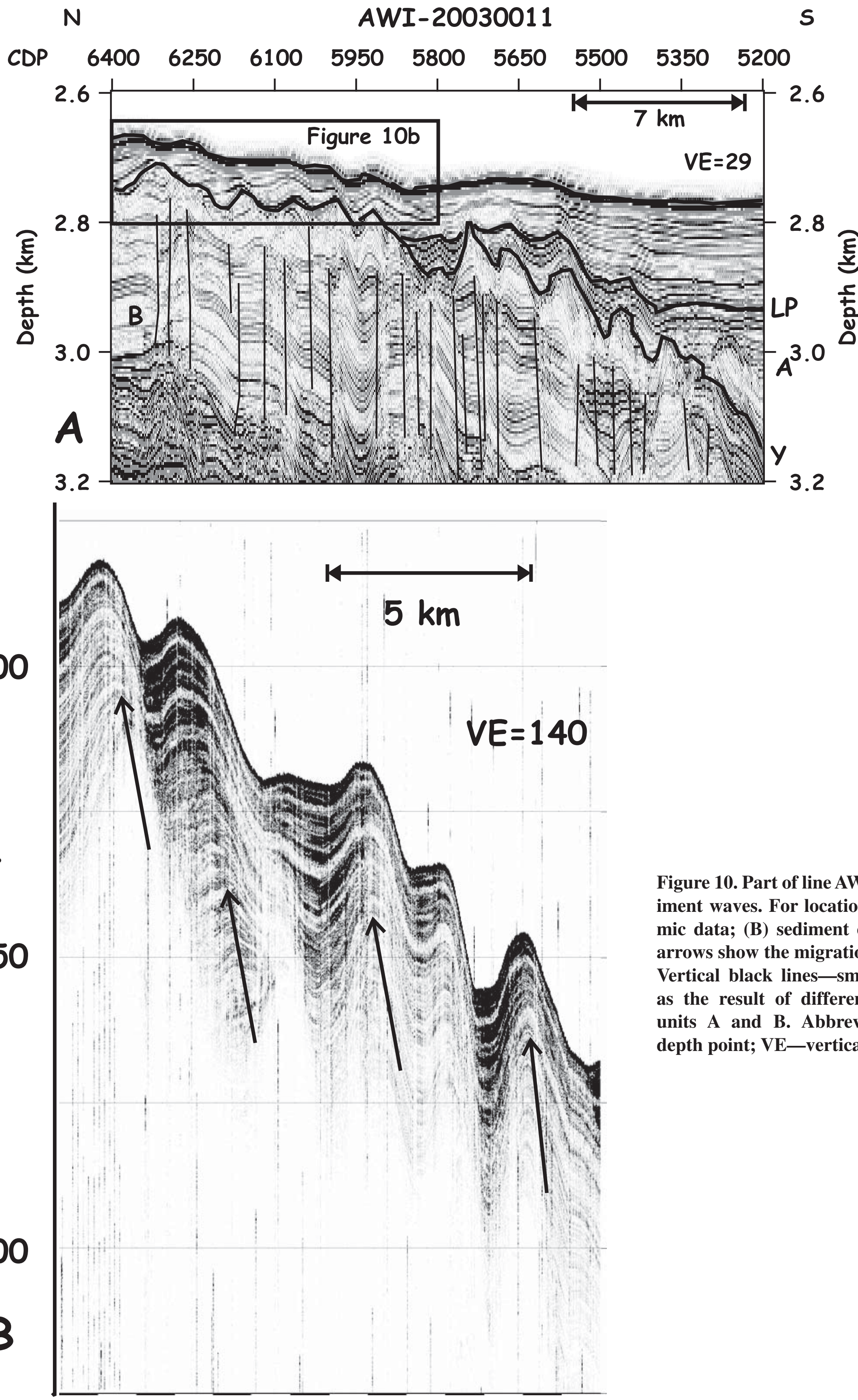

Figure 10. Part of line AWI-20030011 showing sediment waves. For location, see Figure 2. (A) Seismic data; (B) sediment echo-sounding data. The arrows show the migration of the sediment waves. Vertical black lines—small-scale faults probably as the result of differential compaction; A/B—units A and B. Abbreviations: CDP—common depth point; VE—vertical exaggeration.

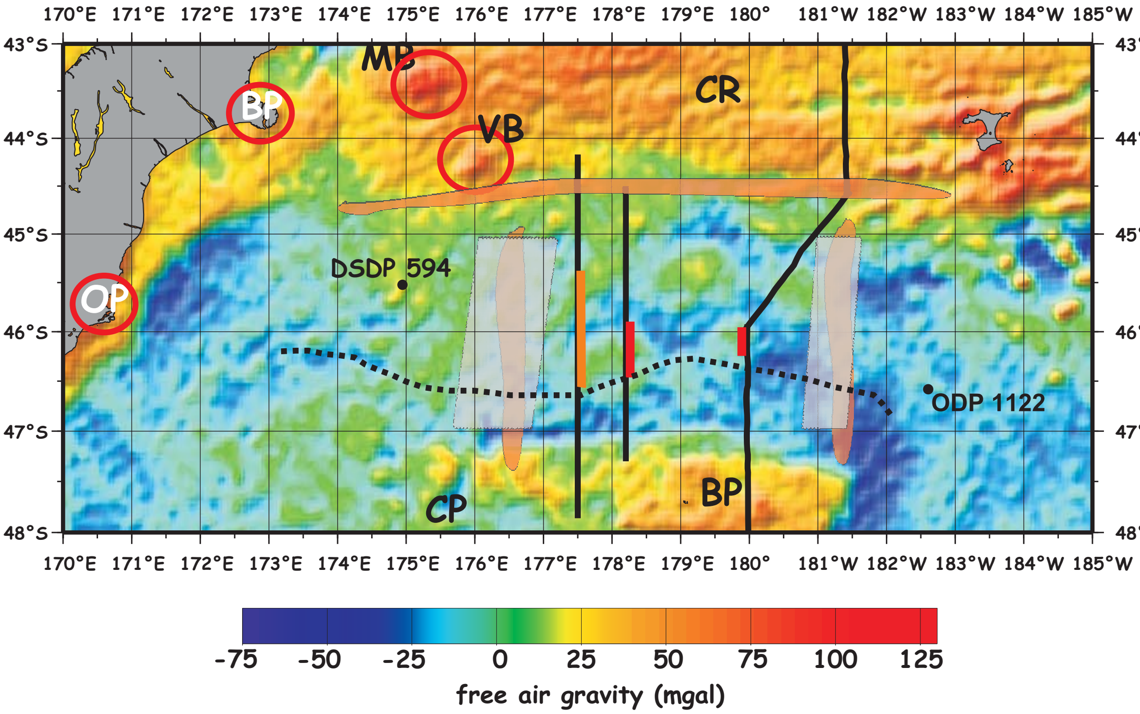

Figure 11. Satellite-derived gravity map of the Bounty Trough (Smith and Sandwell, 1997). Reddish colors refer to positive, bluish colors to negative anomalies. The black lines represent the seismic lines with the red lines showing the locations of the magmatic structures. The dotted line shows the trace of the Bounty Channel. The red circles show the magmatic structures Veryan Bank (VB), Mernoo Bank (MB), Otago Peninsula (OP), and Banks Peninsula (BP). The shaded areas represent the bathymetric steps D1 and D2 of Davy (1993) and the orange, elongated structures the Inner and Outer Sills and the Chatham Sill (in the north). BP—Bounty Platform, CP—Campbell Plateau, CR—Chatham Rise. DSDP—Deep Sea Drilling Project.

current activity on the shelf and slope of the head of Bounty Trough at ca. 12 Ma.

Following the arguments of Carter et al. (1994), we conclude that the basement highs observed in our seismic data are related to late Miocene magmatic activity. The source for the magmatic material remains an enigma. Dredged volcanic samples from the eastern New Zealand continental margin, Banks and Otago Peninsulas have been analyzed with respect to their age and geochemistry, and most samples were found to be younger than 40 Ma (Werner, 2005, personal commun.; Hoernle et al., 2006). Neither age nor spatial pattern could be identified. Werner (2005, personal commun.) and Hoernle et al. (2006) found three types of sources (a high-μ [HIMU]-type mantle source, an enriched mantle [EM]-type source, and a mid-ocean ridge basalt [MORB]-type mantle source, which plays a minor role) in the formation of the Cenozoic magmas, and rule out a simple formation by mantle plumes or extensional tectonics. Instead, they suggest that the first-order cause of melting is decompression melting of upwelling asthenosphere in the garnet stability field, triggered by the removal (detachment) of different parts of the subcontinental lithosphere keel throughout the Cenozoic.

Finn et al. (2005) and references therein discuss a slab detachment model. The subducting slab is detached and deflected horizontally. This slab is gravitationally unstable and capable of triggering episodes of mixing and whole mantle flow. They suggest that the continental alkaline magmatism observed in Australia and New Zealand has its origin in this process starting ca. 55 Ma. Two subduction zones around New Zealand may be considered: the Hikurangi Plateau subduction and the Australian Plate subduction. The subduction of the Australian Plate under the South Island is too young. It began ca. 14 Ma and thus cannot have had an effect at 40 Ma. The subduction of the Hikurangi Plateau under the Chatham Rise has been an ongoing process since the late Cretaceous (Wood and Davy, 1994). Today, the plateau is subducting beneath the North Island. This redirected subduction may constitute the origin of a slab, which triggered episodes of melting beneath eastern New Zealand.

On the basis of our seismic data alone we cannot decide which process of the two presented (decompression melting versus detached slab) is the one actually active east of New Zealand. Still, both models propose an ongoing magmatism without the feasibility to predict future locations of eruptions and/or intrusions. This characterizes the eastern New Zealand continental margin as unstable.

SEDIMENTARY REGIME

We have seen that except for a few locations (Fig. 2, CDPs 4300–4800; Fig. 3, CDPs 3600–4700), sedimentary units D and C mainly drape the basement topography (expressed via onlap and a leveling) and fill depressions between smaller highs. Both reflectors W and X show erosion. Reflector X has been correlated with the Marshall Paraconformity (Carter et al., 1994). Fulthorpe et al. (1996) suggested this paraconformity to have been a result from increased current activity, e.g., due to the evolving Antarctic Circumpolar Current.

Increased current activity is also documented in the deposition of the sediment drifts observed in lower unit B at the slope of Chatham Rise (Figs. 5A, 8, and 9), the northern basement high

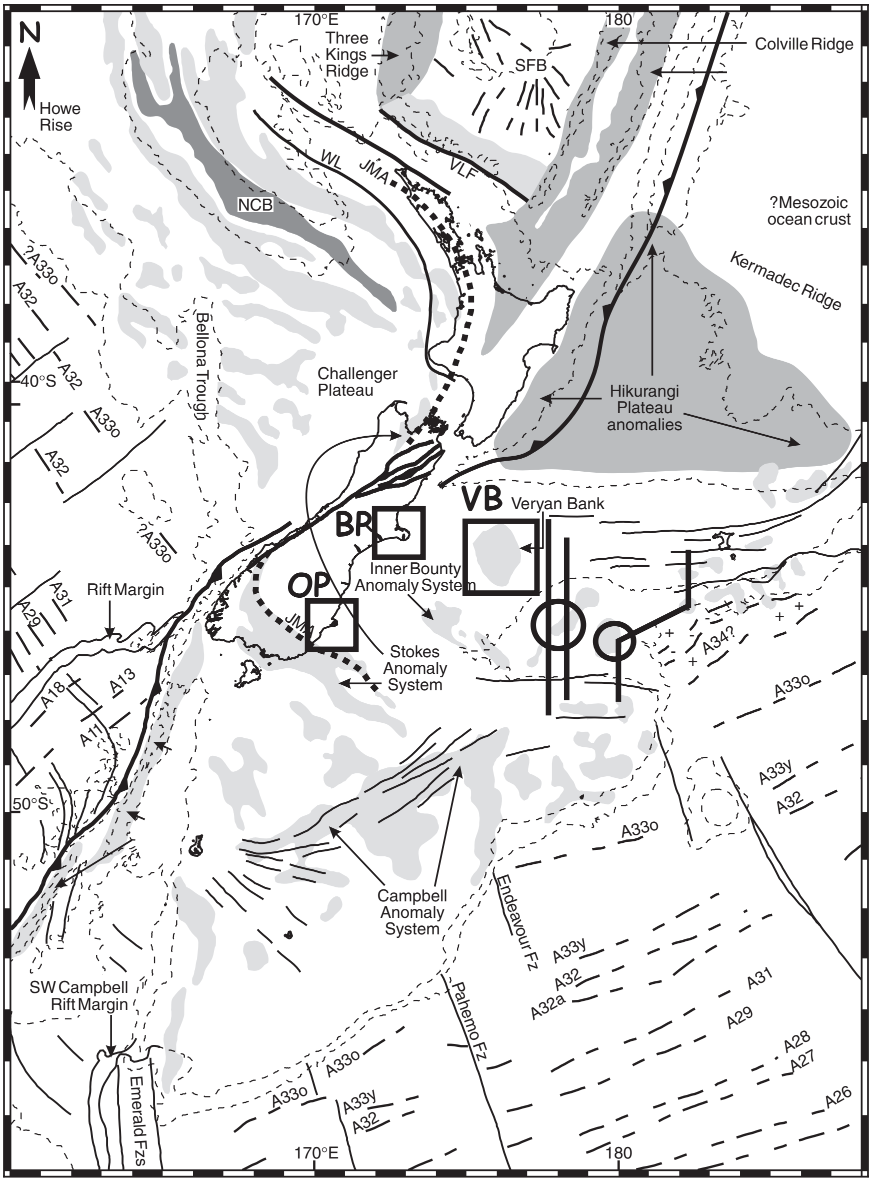

Figure 12. Sketch map of magnetic features (shaded) around New Zealand. The bold lines show the locations of our seismic lines and the bold circles the locations of the observed basement highs. Additionally, the magmatic structures at Veryan Bank (VB), Otago Peninsula (OP), and Banks Peninsula (BP) are marked by bold squares. The dashed lines show the 3000 m and 4000 m water depth contours. Modified from Sutherland (1999). NCB—New Caledonia Basin; SFB—South Fiji Basin.

on line AWI-20030002 (Figs. 5A, 8, and 9), and the basement high north of Bounty Channel (Figs. 5A, 8, and 9). Those drift structures, their location and type (patched-drift; Reeder et al., 2002; Stow et al., 2002) point toward a bottom current that had its path in the central Bounty Trough, north of today's Bounty Channel. This implies that the flow of bottom water was not as restricted and/or more variable than today's flow through Bounty Channel. A paleochannel would be an indication for a restricted paleobottom current. The depression between two basement highs on line AWI-20030002 may be considered to represent this paleochannel (Fig. 3, CDPs 4700–5500), but we don't observe a typical erosion cutting deep into the older layers. The older units C and D show the same topography and a consistent thickness across the high-depression-high structure, which rather indicates a deformation. No levees or overbank deposits can be identified, and the depression shows no infill in either unit B or unit A. Furthermore, there is no indication of a paleochannel on line AWI-20030011, which is located slightly downstream from line AWI-20030002 (Figs. 1 and 2). Small-scale faulting indicates rapid deposition for especially the younger part of unit B. Levees or overbank deposits in connection with the channels cannot be observed; hence we cannot identify a location for a paleo-Bounty Channel.

We observe a larger sediment drift within upper unit B with a moat at the slope toward Chatham Rise (Figs. 2 and 3). This change in drift structure and distribution from two smaller drifts at the trough flanks to a larger one more in the center indicates a reorganization of bottom current flow from the center to the northern and southern rim of the trough at roughly the Oligocene–Miocene boundary, thus eroding the moat at the Chatham Rise slope and starting to cut Bounty Channel. The chaotic zones in the vicinity of today's Bounty Channel (Fig. 5A) may be interpreted as infilling drifts (Damuth and Olsen, 2001) and may hence show old, abandoned and filled locations of Bounty Channel.

Fulthorpe and Carter (1991) as well as Lu et al. (2003) observe sediment drifts in early Miocene to Recent sediments of the Canterbury Basin, which in part form the shelf and slope of the head of Bounty Trough. They see the origin of those drifts in interaction of the Southland Current and a local gyre associated with the Subantarctic Front (SAF) (Fig. 1). The gyre originates in the Antarctic Circumpolar Current and, where it breaks off to the east, leaks across Campbell Plateau. The gyre then recirculates clockwise around the head of Bounty Trough. The sediment drifts in the Canterbury Basin show that the Miocene and Pliocene hydraulic regime was at least as active as the present Southland Current (Lu et al., 2003). Lu et al. (2003) assume that drift formation was linked to enhanced changes in sea level, current strength, and sediment supply caused by two major cooling events (12.5–11.5 Ma and 11–9 Ma), which were identified in the southwest Pacific (Kennett and van der Borch, 1986).

The occurrence of channels, erosion, sediment drifts, and sediment waves in unit B observed in our data most likely is related to the same oceanographic and climatic changes Lu et al. (2003) identified in their data and documents the strong influence that current regime has had on the depositional environment in Bounty Trough at least since the Miocene. The sediment drifts in the lower part of unit B even point to bottom current activity already in Oligocene times, as demonstrated also for shallow marine sections in onland New Zealand by Carter et al. (1996).

Sediment waves observed in upper unit B and unit A show a migration toward the north. This indicates that their buildup is related to east-setting bottom current flow (Viana, 2001). Assuming the major flow is directed through Bounty Channel, we also can infer eastward-directed bottom current flow of significant intensity within the main Bounty Trough.

CONCLUSION

The depositional environment of Bounty Trough was subject to more than one influence in the Neogene. In our seismic data we could identify two major processes that shaped the sedimentary sequences: magmatic activity and bottom current activity.

We have found strong indications for magmatic activity commencing in Miocene times. This resulted in deformation of sedimentary sequences D to B observed by us for the Middle Bounty Trough. We link this observation to widespread magmatic activity as presented by Wood et al. (1989) and Hoernle et al. (2006). Unfortunately, our data can only describe the occurrence of magmatic features and cannot shed light on the origin of the magmatic material.

The second major process shaping the sedimentary units is bottom current activity. The sediments of unit B (middle Oligocene–late Miocene) show the first signs of this process (strong erosion, channels, infill structures, sediment drifts, and sediment waves). Unit A is further affected by it. The oldest signs for the Bounty Channel were identified in unit B. Oligocene–Miocene was thus a period of major modifications in sedimentation processes from magmatic to rather current controlled. Major cooling events in connection with the glaciation of Antarctica in Miocene times led to modifications in the oceanographic regime east of New Zealand. Our new seismic data clearly document the effect of this reorganization.

Bounty Trough represents a good example of the impact that the modifications in climate and oceanographic regime during the Oligocene–Miocene had on the depositional environment. In particular, a former predominantly magmatically shaped depositional system changed into a current controlled regime.

ACKNOWLEDGMENTS

We are grateful for the support of the captain and the crew of RV *Sonne,* who helped us enormously during the expedition. We further want to thank Dr. B. Davy for fruitful discussions. We acknowledge with gratitude the careful and helpful comments of the Associate Editor D. Eaton and the reviewers R. Carter and A. Gorman. This is Alfred Wegener Institute contribution No. awi-n17096. The work was funded by the Bundesministerium für Bildung, Forschung und Technologie under Contract No. 03G0169A.

REFERENCES CITED

Carter, R.M., 1988, The nature and evolution of deep-sea channel systems: Basin Research, v. 1, p. 41–54, doi: 10.1111/j.1365-2117.1988.tb00004.x.

Carter, R.M., and Carter, L., 1988, Late Quaternary development of left-bank-dominant levees in the Bounty Trough, New Zealand: Marine Geology, v. 78, p. 185–197, doi: 10.1016/0025-3227(88)90108-9.

Carter, R.M., and Carter, L., 1996, The abyssal Bounty Fan and lower Bounty Channel: Evolution of a rifted-margin sedimentary system: Marine Geology, v. 130, p. 181–202, doi: 10.1016/0025-3227(95)00139-5.

Carter, R.M., Carter, L., and Davy, B., 1994, Seismic stratigraphy of the Bounty Trough, south-west Pacific Ocean: Marine and Petroleum Geology, v. 11, p. 79–93, doi: 10.1016/0264-8172(94)90011-6.

Carter, R.M., Carter, L., and McCave, I.N., 1996, Current controlled sediment deposition from the shelf to the deep ocean: The Cenozoic evolution of circulation through the SW Pacific gateway: Geologische Rundschau, v. 85, p. 438–451, doi: 10.1007/BF02369001.

Carter, R.M., McCave, I.N., Richter, C., Carter, L., et al., 1999, Site 1122: Turbidites with a contourite foundation, *in* Carter, R.M., McCave, I.N., Richter, C., and Carter, L., et al., eds., Proceedings of the Ocean Drilling Program, Initial reports: Vol. 181: College Station, Texas, Ocean Drilling Program.

Damuth, J.E., and Olsen, H.C., 2001, Neogene-Quaternary contourite and related deposition on the West Shetland Slope and Faeroe-Shetland Channel revealed by high-resolution seismic studies: Marine Geophysical Researches, v. 22, p. 369–399, doi: 10.1023/A:1016395515456.

Davy, B., 1993, The Bounty Trough—Basement structure influences on sedimentary basin evolution, *in* Balance, P.F., ed., South Pacific sedimentary basins: Sedimentary basins of the World, Vol. 2: Amsterdam, Elsevier, p. 69–92.

Finn, C.A., Müller, R.D., and Panter, K.S., 2005, A Cenozoic diffuse alkaline magmatic province (DAMP) in the southwest Pacific without rift or plume origin: Geochemistry Geophysics Geosystems, v. 6, doi: 10.1029/2004GC000723.

Fulthorpe, C.S., and Carter, R.M., 1991, Continental-shelf progradation by sediment-drift accretion: Geological Society of America Bulletin, v. 103, p. 300–309, doi: 10.1130/0016-7606(1991)103<0300:CSPBSD>2.3.CO;2.

Fulthorpe, C.S., Carter, R.M., Miller, K.G., and Wilson, J., 1996, Marshall Paraconformity: A mid-Oligocene record of inception of the Antarctic Circumpolar Current and coeval glacio-eustatic lowstand?: Marine and Petroleum Geology, v. 13, p. 61–77, doi: 10.1016/0264-8172(95)00033-X.

Grobys, J.W.G., Gohl, K., Davy, B., Uenzelmann-Neben, G., Deen, T.J., and Barker, D., 2007, Is the Bounty Trough off eastern New Zealand an aborted rift?: Journal of Geophysical Research, v. 112, doi: 10.1029/2005JB004229.

Hoernle, K., White, J.D.L., van den Bogaard, P., Hauff, F., Coombs, D.S., Werner, R., Timm, C., Garbe-Schönberg, D., Reay, A., and Cooper, A.C., 2006, Cenozoic intraplate volcanism on New Zealand: Upwelling induced by lithospheric removal: Earth and Planetary Science Letters, v. 248, p. 350–367, doi: 10.1016/j.epsl.2006.06.001.

Kennett, J.P., and van der Borch, C.C., 1986, Southwest Pacific Cenozoic paleoceanography, *in* Blakeslee, J.H., ed., Initial report of the Deep Sea Drilling Project, v. 90: Washington, D.C., U.S. Government Printing Office, p. 1493–1517.

Lee, G.H., Kwon, Y.I., Yoon, C.S., Kim, H.J., and Yoo, H.S., 2006, Igneous complexes in the eastern Northern South Yellow Sea Basin and their implications for hydrocarbon systems: Marine and Petroleum Geology, v. 23, p. 631–645, doi: 10.1016/j.marpetgeo.2006.06.001.

Lu, H., Fulthorpe, C.S., and Mann, P., 2003, Three-dimensional architecture of shelf-building sediment drifts in the offshore Canterbury Basin, New Zealand: Marine Geology, v. 193, p. 19–47, doi: 10.1016/S0025-3227(02)00612-6.

McCave, I.N., and Carter, L., 1997, Recent sedimentation beneath the Deep Western Boundary Current off northern New Zealand: Deep-Sea Research, Part I, Oceanographic Research Papers, v. 44, p. 1203–1237, doi: 10.1016/S0967-0637(97)00011-3.

Reeder, M.S., Rothwell, G., and Stow, D.A.V., 2002, The Sicilian gateway: Anatomy of the deep-water connection between East and West Mediterranean basins, *in* Stow, D.A.V., Pudsey, C.J., Howe, J.A. and Viana, A.R., eds., Deep-water contourite systems: Modern drifts and ancient series, seismic and sedimentary characteristics: Geological Society of London, Memoirs, v. 22, p. 171–190.

Selly, R.C., 1997, Elements of petroleum geology: London, Academic Press, 470 p.

Shipboard Scientific Party, 1986, Site 594, *in* Kennett, J.P., ed., Initial reports of the Deep Sea Drilling Project, v. 90: Washington, D.C., U.S. Government Printing Office, p. 653–678.

Smith, W.H.F., and Sandwell, D.T., 1997, Global seafloor topography from satellite altimetry and ship depth sounding: Science, v. 277, p. 1956–1962, doi: 10.1126/science.277.5334.1956.

Stewart, A.A., Harvey, M.J., Otto., S.C., and Weston, P.J., 1996, Influence of salt on fault geometry: Examples from the UK salt basins, *in* Alsop, G.I., Blundell, D.J., and Davison, I., eds., Salt tectonics: Geological Society of London, Special Publication, v. 100, p. 175–202.

Stow, D.A.V., Faugeres, J.-C., Howe, J.A., Pudsey, C.J., and Viana, A.R., 2002, Bottom currents, contourites and deep-sea sediment drifts: Current state-of-the-art, *in* Stow, D.A.V., Pudsey, C.J., Howe, J.A., and Viana, A.R., eds., Deep-water contourite systems: Modern drifts and ancient series, seismic and sedimentary characteristics: Geological Society of London, Memoirs, v. 22, p. 7–20.

Sutherland, R., 1999, Basement geology and tectonic development of the greater New Zealand region: An interpretation from regional magnetic data: Tectonophysics, v. 308, p. 341–362, doi: 10.1016/S0040-1951(99)00108-0.

Uenzelmann-Neben, G., 2001, Seismic characteristics of sediment drifts: An example from the Agulhas Plateau, southwest Indian Ocean: Marine Geophysical Researches, v. 22, p. 323–343, doi: 10.1023/A:1016391314547.

Uenzelmann-Neben, G., Gohl, K., Ehrhardt, A., and Seargent, M., 1999, Agulhas Plateau, SW Indian Ocean: New evidence for excessive volcanism: Geophysical Research Letters, v. 26, p. 1941–1944, doi: 10.1029/1999GL900391.

Viana, A.R., 2001, Seismic expression of shallow- to deep-water contourites along the south-eastern Brazilian margin: Marine Geophysical Researches, v. 22, p. 509–521, doi: 10.1023/A:1016307918182.

Wood, R., and Davy, B., 1994, The Hikurangi Plateau: Marine Geology, v. 118, p. 153–173, doi: 10.1016/0025-3227(94)90118-X.

Wood, R.A., Andrews, P.B., Herzer, R.H., et al., 1989, Cretaceous and Cenozoic geology of the Chatham region, South Island, New Zealand: New Zealand Geological Survey Basin Studies, v. 3, p. 1–76.

Yilmaz, Ö., 2001, Seismic data analysis: Investigations in geophysics, no 10: Tulsa, Society of Exploration Geophysicists, 2027 p.

Manuscript Received 4 May 2007
Revised Manuscript Received 1 April 2008
Manuscript Accepted 2 April 2008

Printed in the USA